

Beamline AR-NW12A: high-throughput beamline for macromolecular crystallography at the Photon Factory

L. M. G. Chavas,^{a*} N. Matsugaki,^a Y. Yamada,^a M. Hiraki,^a N. Igarashi,^a M. Suzuki^b and S. Wakatsuki^a

^aStructural Biology Research Center, Photon Factory, High Energy Research Organization, 1-1 Oho, Tsukuba, Ibaraki 305-0801, Japan, and ^bInstitute for Protein Research, Osaka University, Osaka 565-0871, Japan.
E-mail: leonard.chavas@kek.jp

AR-NW12A is an in-vacuum undulator beamline optimized for high-throughput macromolecular crystallography experiments as one of the five macromolecular crystallography (MX) beamlines at the Photon Factory. This report provides details of the beamline design, covering its optical specifications, hardware set-up, control software, and the latest developments for MX experiments. The experimental environment presents state-of-the-art instrumentation for high-throughput projects with a high-precision goniometer with an adaptable goniometer head, and a UV-light sample visualization system. Combined with an efficient automounting robot modified from the SSRL SAM system, a remote control system enables fully automated and remote-access X-ray diffraction experiments.

© 2012 International Union of Crystallography
Printed in Singapore – all rights reserved

Keywords: macromolecular crystallography; high-throughput experiment; automated data collection; remote access; sample exchange robot.

1. Introduction

Located on the campus of the High Energy Accelerator Research Organization (KEK), the Photon Factory (PF) storage ring and the PF Advanced Ring (PF-AR) are operated as two synchrotron light sources. The PF-AR is a 6.5 GeV ring that was commissioned in 1984, converted to a dedicated synchrotron radiation source in 1998, and greatly upgraded in 2001. It currently accommodates eight beamlines, including the insertion-device beamline AR-NW12A, the oldest macromolecular crystallography (MX) beamline presently operational at KEK. AR-NW12A was constructed as an MX beamline mostly from an initial USD 6 million project as part of the 2001 upgrade scheme of the PF-AR Northwest Experimental Hall. The beamline was commissioned and then opened to users in May 2003, and has been operating as a high-throughput end-station since then. Academic users are being accommodated about 60% of the overall beam time available for the MX beamlines after being peer-reviewed by the PF Program Advisory Committee (PF-PAC). In recent years the number of users visiting MX beamlines has steadily increased, which can be reflected at AR-NW12A where 132 days of beam time were assigned in 2010, corresponding to a 36% gain compared with 2005.

2. Beamline overview

AR-NW12A is an MX beamline located at the PF-AR 6.5 GeV synchrotron source. The beamline was originally implemented as a high-throughput MX end-station, and subsequently equipped to accept multiple types of experimental environments, such as data collection of crystals with a size going down to 50 μm , crystals with

large cell dimensions, and multiple/single-wavelength anomalous dispersion (MAD/SAD) experiments, and was recently expanded to adapt high-pressure crystallography set-ups (Nagae *et al.*, 2012). AR-NW12A accepts 0.312 mrad (horizontal) \times 0.029 mrad (vertical) of a 1.57 mm \times 0.17 mm beam from a U#NW12 in-vacuum undulator comprising 95 periods, each of length 40 mm, and which can be operated at a minimum gap of 10.0 mm with $B_{\text{eff}} = 0.8$ T. The sample position is located at 38.1 m from the light source, and exposed by a monochromatic beam in the energy range 6.5–17.7 keV with an energy resolution of about 2.5×10^{-4} (Table 1). The flux measured at the sample position at 12.39 keV is about 2.9×10^{11} photons s^{-1} for a typical beam size of 200 μm \times 200 μm . Developed below are brief descriptions of each element along the beam path downstream of the undulator and up to the area detector, as shown in Fig. 1.

2.1. Interlock system and beam position monitors

A strict communication between a simple transmission and retrieval system (STARS) protocol-based beamline interlock control system (BLIS) (Kosuge *et al.*, 2000) and the ring status allows a perfectly secured control of the beamline front-end, and notably of the main beam shutter (MBS). The BLIS checks each of the optical components in terms of temperature and vacuum level, and permits the opening of the MBS and subsequently of the downstream beam shutter (DSS) only if all the conditions are confirmed to be safe.

A set of horizontal and vertical wire monitors (H/VWM), five fluorescent screens (FS1–FS5), one gas-filled ion chamber (IC) and a silicon photodiode (PD) are arranged along the beam path. The H/VWMs and FSs are retractable and employed exclusively for beamline alignment purposes, to monitor the relative positions of the white

Table 1

Beamline details.

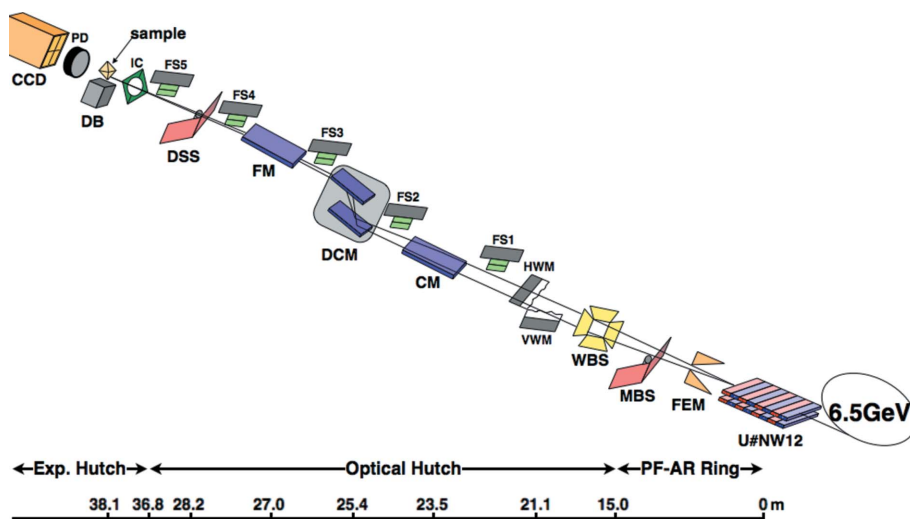
Beamline name	AR-NW12A
Source type	In-vacuum undulator
Mirrors	1 m Rh-coated Si flat (CM) and toroidal (FM)
Monochromator	Double-crystal Si(111) liquid-nitrogen-cooled
Energy range (keV)	6.5–17.7
Wavelength range (Å)	0.7–1.9
Beam size (uncollimated) (μm) [†]	800 × 200
Beam size (collimated, typical) (μm) [†]	200 × 200
Flux (uncollimated) (photons s ⁻¹) [†]	2.2 × 10 ¹²
Flux (collimated, typical) (photons s ⁻¹) [†]	2.9 × 10 ¹¹
Goniometer	Single-axis ball bearing
Cryo capability	Rigaku GN2; liquid nitrogen available
Sample mounting	PAM
Detector type	Fiber-optic coupled CCD
Detector model	ADSC Quantum 210r
2 Θ capabilities	None; vertical offset 110 mm

[†] Measurements were performed on a silicon photodiode at 12.39 keV with the third harmonic of the U#NW12 at a ring current of 60 mA.

beam and subsequently of the monochromatic beam (Fig. 1). Measurement of the flux is performed online using the IC located prior to the sample position, and the PD mounted on a retractable X-ray CCD detector shield, the latter being used only for fine beam alignments.

2.2. Mirrors and monochromator

Downstream from the white-beam slits (WBS) is located a vertical single-crystal collimating mirror (CM, flat shaped, 1 m long, rhodium-coated silicon) with a glancing angle of 3.5 mrad. Through mechanical bends, the water-cooled CM is used to collimate the incoming beam to the double-crystal monochromator (DCM), and diminishes in the meantime the heat load on the first crystal of the DCM generated by the 6.5 GeV PF-AR white beam. The collimated beam then passes through both crystals of the DCM prior to being focused by a toroidal single-crystal focusing mirror (FM, 1 m long, rhodium-coated silicon)


Figure 1

Beamline layout with relative distances (not to scale) from the light source. U#NW12, in-vacuum undulator NW12; FEM, front-end beam-defining mask; MBS, main beam shutter; WBS, white-beam slits; H(V)WM, horizontal (vertical) wire monitor; FS, fluorescent screen; CM, collimating mirror; DCM, double-crystal monochromator; FM, focusing mirror; DSS, downstream shutter; IC, ion chamber; DB, diffractometer box; PD, photodiode; CCD, X-ray CCD detector.

with a glancing angle of 3.5 mrad. The focus point at the sample position is located at 11.1 m from the FM (demagnification of 2.44), and 38.1 m from the light source (Fig. 1). The DCM at AR-NW12A [numerical link type Si(111) crystals] was favored over other types of monochromators principally owing to its ease of use and capacity of maintaining the offset between the incoming and outgoing beam only by changing the gap between the two crystals when varying the energy. The two crystals are cooled using liquid nitrogen through an inline liquid-nitrogen cooling system (Suzuki Shokan) that allows an efficient temperature control and rapid response to changing heat loads.

Although most of the power of the strong incoming white beam is absorbed by the CM, and because of the current decrease of the PF-AR storage ring, the heat load on the first crystal of the DCM varies with time, causing changes in the crystal shape with local deformations, which is generally characterized by a shift in the beam height at the sample position. To limit this notorious effect, a piezo-electric device coupled with a beam-position feedback system was installed below the first DCM crystal. More precisely, a software-based feedback loop calculates the position of the beam passing through the IC and generates a proportional error signal digitally outputted to the piezo-controller (E-501.00; PI-Piezo) that in turn moves the piezo-motor (P-239.3SV; PI-Piezo) via a closed loop. This implementation allows continuous diffraction experiments for 12 h between beam injections with the beam position that remains unchanged within 20 μm .

2.3. Experimental environment

The experimental environment at AR-NW12A can be divided into three distinct areas. When arriving in the experimental hutch, the monochromatic beam is probed for its intensity and position by the IC, directly linked to the piezo-electric-based feedback system on the DCM to keep a constant beam position. Exiting from the IC, the beam passes through a beam attenuation unit, which consists of a series of aluminium foils of various thickness displayed on a motorized disk that provides an attenuated X-ray beam ranging from 0.1% to 100% depending on the beam energy. After the attenuator and preceding the beam shutter, two sets of quad-slits are used to shape the beam (typical size 200 μm × 200 μm).

Regrouped in a single box, most of the experimental environment apparatus directly operated by the users is arranged near the sample position (Fig. 2). Basically, all the various parts are retractable and can be mounted on demand, respecting some rules as to avoiding collision with other components. For instance, during data collection, the cryo-nozzle (CN), the guard slit (GS) and direct beam stopper (BS) are mounted, directly surrounding the sample; for EXAFS experiments a Si-PIN diode X-ray fluorescence detector (FD) comes near the sample, together with the GS; during crystal alignment, all components but the cold-light (CL) and eventually the UV-light (UVL) are removed. The GS removes unwanted parasitic scattering, and is made of a tantalum plate presenting a pinhole of 600 μm at its center. Downstream of the sample, two direct X-ray beam stoppers are

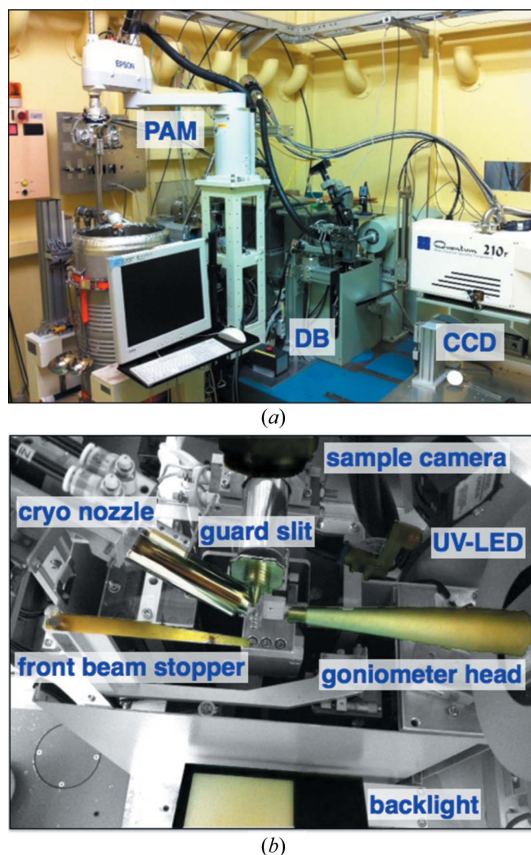


Figure 2
 (a) Experimental hutch viewed from the user's side. (b) Top view of the experimental environment, with the X-rays coming from above, as met during data collection.

provided. The front beam stopper (FBS) is mounted on a slender metal arm and aligned with the rotation axis to place the arm shadow within the cusp of the diffraction pattern. For particular set-ups that necessitate the full access of the space surrounding the sample position, such as the implementation of a diamond anvil cell (DAC) for high-pressure studies, a rear beam stopper (RBS) built as a fixed frame on the X-ray CCD detector is also available. Crystal centering is facilitated by a high-power (150 W) CL light emitted from a large flat panel, which has been optimized to allow visualization of the samples even during data collection without interfering with the diffraction experiment. A low-power (0.5 mW) 280 nm UVL can be mounted to help in the identification of the crystals [Fig. 3(a); Chavas *et al.*, 2011]. The samples are cooled by a flow of cold nitrogen gas coming out of a GN2 cryo-system (Rigaku) that allows working under cryo-conditions down to 95 K. According to the operation requested, the distance between the sample and the exit of the CN is remotely controlled while keeping the temperature at the sample position unchanged.

Ensuring the proper alignment of the sample at the beam position, a cylinder of confusion of 2 μm is achieved with rotations around a single axis of a goniometer (Kohzu Precision). The adaptable goniometer head allows different types of sample holder to be accepted, including DACs (Chervin *et al.*, 1995) for high-pressure experiments [Figs. 3(c)–3(d)]. Diffraction patterns are recorded on a Quantum 210r X-ray CCD camera (ADSC), with a sample-to-camera distance ranging from 60 to 950 mm. The CCD can be shifted vertically by 110 mm for high-resolution data collection up to 0.85 Å at a wavelength of 1 Å (Fig. 3b).

3. Ancillary facilities

All of the beamline control and data processing is performed from a control cabin, located adjacent to the experimental hutch. The cabin is also equipped with benches, microscopes and cryo-tools for sample preparation. An external laboratory is also at the disposition of the users, equipped with two temperature-controlled areas (277 and 293 K) for long-time sample conservation.

To favor an easy sample manipulation, a Stanford Synchrotron Radiation Lightsource (SSRL)-type mounting robot (Cohen *et al.*, 2002) called PAM ('PF automated mounting robot') was implemented at all the PF MX beamlines, and was recently upgraded to adapt the Gemini double-tongue system (Hiraki *et al.*, 2008) and Universal pucks (Unipuck). By taking advantage of a large sample storage dewar, PAM is capable of mounting a total of 288 samples (3 SSRL cassettes of 96 sample holders) or 192 samples (12 Unipuck cassettes of 16 sample holders) continuously and undisturbed, without the need to access the experimental hutch. With an optimized data collection scheduling, and with the robot working at full regime, the sample exchange time goes down to 10 s (Hiraki *et al.*, 2007).

All of the beamline components can be controlled *via* a unified GUI (UGUI) software developed on site. The software is constantly being ameliorated, and is implemented at all of the PF MX beamlines in a will to help users working in a friendly and exportable environment. UGUI is a Perl script base software that takes advantage of the STARS communication protocol to control all the hardware components of the beamline. Additionally, data processing and analysis software commonly used by protein crystallographers are available, including *HKL2000* (Otwinowski & Minor, 1997), *iMosflm* (Battye *et al.*, 2011), *XDS* (Kabsch, 1993), *CCP4i* (Collaborative Computational Project, Number 4, 1994), *PHENIX* (Adams *et al.*, 2002), *SHELX* (Sheldrick, 2008) and other related programs.

4. Facility access

Evaluated based on their scientific merit and technical feasibility of the research plan, beam time application proposals to public beamlines of the PF can be submitted twice a year. Proposals are first reviewed by referees, and subsequently by members of the PF-PAC, who assign a ranking score used for prioritizing allocations.

For remote-access experiments, a dedicated so-called 'external mode' has been implemented at AR-NW12A. The external mode takes advantage of the strict communication protocol that exists between the beamline shutters and the ring status through the BLIS to permit a safe control of the beamline. In addition, by accessing the UGUI beamline control software *via* a unique NoMachine NX session, users can fully run the beamline from their home laboratory just as if they were on site. Coupled with the PAM, the external access has obvious advantages for geographically remote users or even for teaching purposes.

5. Highlights

Commissioned in May 2003, AR-NW12A approaches its ten-year anniversary. Since its first users, the beamline has been extensively used both by academic users and pharmaceutical companies. As of January 2012, more than 540 coordinates were deposited in the Protein Data Bank for crystal structures of data collected at the beamline. Presented below is a non-exhaustive list of recent research results from the beamline, highlighting various types of experimental capabilities available at AR-NW12A.

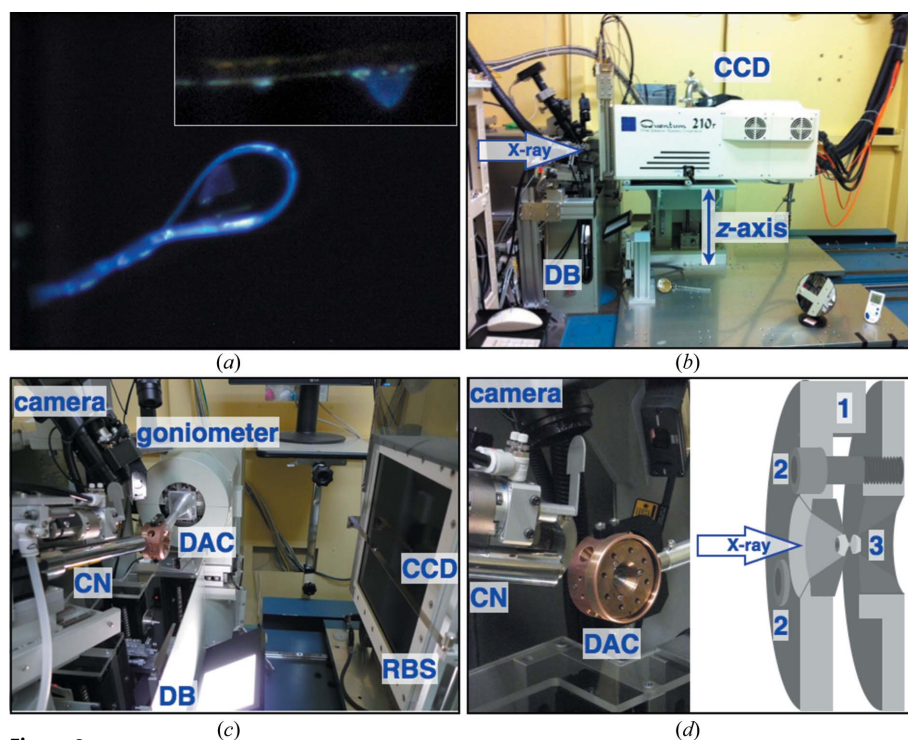


Figure 3
Examples of applications available at AR-NW12A. (a) Crystal samples visualized by the UV-LED backlight system in the case of nylon loops and litholoops (inset). (b) Camera shift in the z -direction for high-resolution data collection. (c) High-pressure crystallography set-up. (d) Zoomed view of the DAC sample holder (left), and a drawing of its construction (right) with (1) tungsten carbide support; (2) spring-loaded screws for high-pressure generation; (3) diamond anvil.

5.1. MAD/SAD: PYL family signal regulator

The pyrabactin resistance-like (PYL) family of proteins are phytohormone abscisic acid (ABA) receptors that inhibit the activity of type-2C protein phosphatases in plants in response to ABA, action required for the proper regulation of the machinery for activating the drought-tolerance response in plants. The structure of the complex PYL-ABA was solved by the MAD method using selenium as the anomalous atom, at a resolution of 2.05 Å (Miyazono *et al.*, 2009). This report is one of numerous studies performed at AR-NW12A that took advantage of MAD and SAD methods for structure determination.

5.2. High resolution: aristaless homeodomain

Accurate gene regulation is partly achieved by cooperative binding to DNA of homeodomain proteins, such as aristaless (AI) or clawless (CII) DNA-binding proteins. To understand the regulation mechanism of such proteins, the ternary complex structure between AI, CII and DNA, and that of the individual homeodomain proteins alone were solved, with the structure of the homeodomain AI that was refined to a resolution of 1.00 Å (Miyazono *et al.*, 2010).

5.3. Large cell constants: bursal disease virus

In infectious bursal disease virus (IBDV), the viral protein VP2 constitutes part of the unenveloped icosahedral capsid and is the primary immunogen. The crystal structure of VP2 was solved and refined at 2.6 Å resolution, providing essential insights into the mechanism by which VP2 spontaneously assembles to form the building block of IBDV (sub)viral particles. In these studies, 20 structurally heterogeneous protein subunits crystallized in the space group $P2_13$, with large cell dimensions of $a = b = c = 316$ Å (Lee *et al.*, 2006).

5.4. High-pressure studies: proteins from deep-sea organisms

Most of the enzymes originating from deep-sea organisms remain active at high pressures while related enzymes from land organisms lose their activity (Kato *et al.*, 2008). To understand the pressure tolerance of proteins from deep-sea organisms, structural studies on several isopropylmalate dehydrogenase (IPDMH) from non-piezophile *S. oneidensis* MR-1 were performed at pressures ranging from atmospheric pressure to 650 MPa using a dedicated DAC (Nagae *et al.*, 2012).

6. Discussion and conclusions

Considering the constant increase of proposal applications and requests for MX beam time, the need to implement fast data collection procedures with stable X-ray beams is of prime importance, and is well achieved at AR-NW12A. By taking advantage of our exceptionally quick and reliable mounting set-up (PAM equipped with the Gemini double-tongue system), the beamline could be fully automated and accept an even greater number of users for a shorter amount of beam time needed. With an averaged exposure time of 2 s per degree, a full data set of 180 frames with 1° oscillation

angle could be collected in less than 10 min. Considering a time of 10 s for sample exchange when using our PAM system, a total of about 140 data sets could be collected in a 24 h shift (taking into account the time necessary to re-align the beam after the electron beam injection that occurs twice a day at PF-AR). The combined operation of the external mode with the remote access will facilitate unassisted data collection experiments from users located outside of the PF, which has clear advantages for geographically remote users.

To ease sample centering, notably during high-pressure experiments, an on-axis visualization system would be of indubitable value. Future developments at the beamline will also see the integration of a fully automated crystal centering procedure that exploits the specific properties of UV light. Together with the implementation of a decision-making strategy within the UGUI beamline control software, these developments will contribute to strengthening a pipeline for full automation of crystallographic experiments at all the PF MX beamlines.

The authors would like to thank the Photon Factory MX beamline crew. A part of this work was supported by Special Coordination Funds for Promoting Science and Technology (JSPS), Protein 3000 Project (MEXT), Targeted Proteins Research Program (MEXT), Grant-in-Aid for Young Scientists (JSPS).

References

- Adams, P. D., Grosse-Kunstleve, R. W., Hung, L.-W., Ioerger, T. R., McCoy, A. J., Moriarty, N. W., Read, R. J., Sacchettini, J. C., Sauter, N. K. & Terwilliger, T. C. (2002). *Acta Cryst.* **D58**, 1948–1954.
- Battye, T. G. G., Kontogiannis, L., Johnson, O., Powell, H. R. & Leslie, A. G. W. (2011). *Acta Cryst.* **D67**, 271–281.

- Chavas, L. M. G., Yamada, Y., Hiraki, M., Igarashi, N., Matsugaki, N. & Wakatsuki, S. (2011). *J. Synchrotron Rad.* **18**, 11–15.
- Chervin, J.-C., Canny, N., Besson, J.-M. & Pruzan, P. (1995). *Rev. Sci. Instrum.* **66**, 2595–2598.
- Cohen, A. E., Ellis, P. J., Miller, M. D., Deacon, A. M. & Phizackerley, R. P. (2002). *J. Appl. Cryst.* **35**, 720–726.
- Collaborative Computational Project, Number 4 (1994). *Acta Cryst.* **D50**, 760–763.
- Hiraki, M., Watanabe, S., pHonda, N., Yamada, Y., Matsugaki, N., Igarashi, N., Gaponov, Y. & Wakatsuki, S. (2008). *J. Synchrotron Rad.* **15**, 300–303.
- Hiraki, M., Watanabe, S., Yamada, Y., Matsugaki, N., Igarashi, N., Gaponov, Y. & Wakatsuki, S. (2007). *AIP Conf. Proc.* **879**, 1924–1927.
- Kabsch, W. (1993). *J. Appl. Cryst.* **26**, 795–800.
- Kato, C., Sato, T., Abe, F., Ohmae, E., Tamegai, H., Nakasone, K., Siddiqui, K. S. & Thomas, T. (2008). *Molecular Anatomy and Physiology of Proteins*, pp. 167–191. New York: Nova Science.
- Kosuge, T., Saito, Y., Nigorikawa, K., Ito, K., Abe, I. & Kurokawa, S. (2000). *International Workshop on PCs and Particle Accelerator Controls (PCaPAC 2000)*.
- Lee, C. C., Ko, T. P., Chou, C. C., Yoshimura, M., Doong, S. R., Wang, M. Y. & Wang, A. H. (2006). *J. Struct. Biol.* **155**, 74–86.
- Miyazono, K., Miyakawa, T., Sawano, Y., Kubota, K., Kang, H. J., Asano, A., Miyauchi, Y., Takahashi, M., Zhi, Y., Fujita, Y., Yoshida, T., Kodaira, K. S., Yamaguchi-Shinozaki, K. & Tanokura, M. (2009). *Nature (London)*, **462**, 609–614.
- Miyazono, K., Zhi, Y., Takamura, Y., Nagata, K., Saigo, K., Kojima, T. & Tanokura, M. (2010). *EMBO J.* **29**, 1613–1623.
- Nagae, T., Kawamura, T., Chavas, L. M. G., Niwa, K., Hasegawa, M., Kato, C. & Watanabe, N. (2012). *Acta Cryst.* **D68**, 300–309.
- Otwinowski, Z. & Minor, W. (1997). *Methods Enzymol.* **276**, 307–326.
- Sheldrick, G. M. (2008). *Acta Cryst.* **A64**, 112–122.